Biosensors and Bioelectronics 24 (2009) 3671–3676

Contents lists available at ScienceDirect

Biosensors and Bioelectronics

journal homepage: www.elsevier.com/locate/bios

Polycrystalline bismuth oxide films for development of amperometric biosensor for phenolic compounds

Dan Shan[a,b], Jing Zhang[a], Huai-Guo Xue[a,b,*], Yong-Cai Zhang[a], Serge Cosnier[c], Shou-Nian Ding[a,c,d]

[a] Key Laboratory of Environmental Materials & Environmental Engineering of Jiangsu Province, Yangzhou 225002, China
[b] School of Chemistry & Chemical Engineering, Yangzhou University, Jiangsu 225002, China
[c] Département de Chimie Moléculaire UMR-5250, ICMG FR-2607, CNRS Université Joseph Fourier, BP-53, 38041 Grenoble, France
[d] School of Chemistry & Chemical Engineering, Southeast University, Nanjing 211189, China

ARTICLE INFO

Article history:
Received 2 May 2009
Accepted 28 May 2009
Available online 6 June 2009

Keywords:
Bismuth oxide film
Inorganic matrix
Polyphenol oxidase
Biosensor

ABSTRACT

An attractive biocomposite based on polycrystalline bismuth oxide (BiO_x) film and polyphenol oxidase (PPO) was proposed for the construction of a mediator-free amperometric biosensor for phenolic compounds in environmental water samples. The phenolic biosensor could be easily achieved by casting the biocomposite on the surface of glassy carbon electrode (GCE) via the cross-linking step by glutaraldehyde. The laboratory-prepared bismuth oxide semiconductor was polymorphism. Its hydrophilicity provided a favorable microenvironment for retaining the biological activity of the immobilized protein. The parameters of the fabrication process and the various experimental variables for the enzyme electrode were optimized. The proposed PPO/BiO_x biosensor provided a linear response to catechol over a concentration range of 4×10^{-9} M to 1.5×10^{-5} M with a dramatically developed sensitivity of 11.3 A M^{-1} cm^{-2} and a detection limit of 1×10^{-9} M based on S/N = 3. In addition, the PPO/BiO_x biocomposite was characterized by scanning electron microscope (SEM), Fourier transform infrared spectra (FTIR) and rotating disk electrode voltammetry.

1. Introduction

Phenolic compounds stemming from various production processes of man-made materials such as plastics, dyes, pesticides, paper and petrochemical products are some of the most important contaminates present in the environment. Many of these compounds and their derivatives are extremely harmful to humans through oral, dermal, or respiratory tracks and thus bring about a serious environmental problem. Hence, the rapid determination of trace phenolic compounds is of great importance for evaluating the total toxicity of an environmental water sample. Several methods, such as spectrophotometry (Lupetti et al., 2004; Oliveira et al., 2005), liquid chromatography (Pocurull et al., 1996; Bagheri et al., 2004), gas chromatography (Bagheri and Mohammadi, 2003; Faraji, 2005), and capillary electrophoresis (Marlow and Hurtubise, 2004) have been described in the literature for detection of phenols in water samples. However, some of these techniques are expensive, time consuming and need skilful operators and sometimes require preconcentration and extraction steps.

Amperometric biosensor based on polyphenol oxidase has been considered to be a promising tool for the detection of phenolic compounds (Liu et al., 2000; Mailley et al., 2003; Shan et al., 2003, 2007; Han et al., 2007; Fan et al., 2007). PPO is a metalloenzyme that contains a binuclear copper active site and catalyzes, in the presence of dioxygen, the hydroxylation of monophenols to catechols (monooxygenase activity), which in turn are oxidized to *o*-quinone (catecholase activity). The phenol biosensor transduction is thus based on the amperometric detection of the enzymatically-generated *o*-quinone. However, few of them were applied to the real water sample determination.

Transition metal oxides are particularly interesting because they are one of the most common transition metal complexes, and they can also exhibit ferroelectric and ferromagnetic ordering (Wagner, 2007; Wagner and Mitas, 2007). Bismuth oxide is one of the important transition metal oxides, which plays a significant role in modern solid-state technology due to its peculiar properties in band gap, refractive index, dielectric properties, etc. These properties extent its application, such as catalysts, optical coatings, photovoltaic cells, microwave integrated circuits, fuel cells, oxygen sensors and oxygen pumps, etc. (Shuk et al., 1996; Fu, 1997; Switzer et al., 1999; Li, 2006; Gujar et al., 2006). In addition, BiO_x is nontoxic and has excellent chemical inertness and biocompatibility. Nanosized bismuth oxide shows greater advantages and novel

* Corresponding author at: School of Chemistry & Chemical Engineering, Yangzhou University, Jiangsu 225002, China. Tel.: +86 514 7975520; fax: +86 514 87975244.
E-mail address: chhgxue@yzu.edu.cn (H.-G. Xue).

0956-5663/$ – see front matter © 2009 Elsevier B.V. All rights reserved.
doi:10.1016/j.bios.2009.05.038

characteristics than regular sized particles, such as the much higher specific surface and greater surface free energy, which are favorable for the biomolecules adsorption. Nevertheless, to our knowledge, bismuth oxide particles have never been used for the construction of a biosensor.

The objective for this study was to develop an amperometric PPO-based biosensor for determination of phenolic compounds in environmental water samples. We used for the first time polycrystalline BiO_x films for the entrapment of biomolecules. This procedure constituted an inexpensive, fast and easy method for the elaboration of enzyme electrodes, by the simple mixing of the colloidal suspension of bismuth oxide with proteins, followed by their deposition on the electrode surface.

2. Experimental

2.1. Reagents

Polyphenol oxidase (PPO) (EC 1.14.18.1) from mushroom (807 units mg^{-1}) was purchased from Amresco (America). All other reagents were of analytical grade and used as received without further purification. All aqueous solutions were prepared in deionized distilled water. Phenolic solutions in 0.1 M phosphate buffer solution (PBS) (pH 6.0) were prepared daily.

2.2. Apparatus

A CHI 660 electrochemical workstation (CHI Co., USA) was used for electrochemical experiments. All electrochemical studies were performed with a conventional three-electrode system. A saturated calomel electrode (SCE) and a Pt foil electrode were used as the reference electrode and the counter electrode, respectively. The working electrode was a glassy carbon electrode (diameter 3 mm), which was polished carefully with 0.05 μm alumina particles on silk and was then rinsed with distilled water and dried in air before use. All measurements were carried out in a thermostated cell at 25 °C, containing phosphate buffer solution. Fourier transform infrared (FT-IR) spectra of the samples were measured on a pressed pellet with KBr, employing a Tensor 27 spectrometer (Bruker, Canada). X-ray powder diffraction patterns were collected on a Bruker D8 advance diffractometer (German) using Cu Kα radiation. Patterns were recorded over the 2θ range 10–80°. Micrographs were obtained with a XL-30E scanning electron microscope (SEM) (Philips, The Netherlands). Static contact angle measurements were performed at 20 °C with a sessile drop method using an OCA 40 system (Dataphysics, German). A droplet of deionized water (2 μl) was gently placed onto the surface. The angle between the edge of the droplet and the surface was measured. Measurements were made in different regions on the surface.

2.3. Bismuth oxide preparation

Bismuth oxide samples were prepared following the previous report (Gotić et al., 2007). Firstly, an aqueous 0.1 M $Bi(NO_3)_3$ solution was prepared as follows: 9.796 g of $Bi(NO_3)_3{\cdot}5H_2O$ was weighted and quantitatively transferred into a 200 ml volumetric flask, followed by the addition of deionized water and drop by drop of concentrated nitric acid, swirling and shaking until the bismuth salt was completely dissolved. $NH_3{\cdot}H_2O$ was added to the bismuth solution until the pH reached a value of 9.0. The suspensions were then autoclaved at 180 °C for 24 h. The precipitates were isolated by repeated washing and centrifugation, and then dried under vacuum at room temperature.

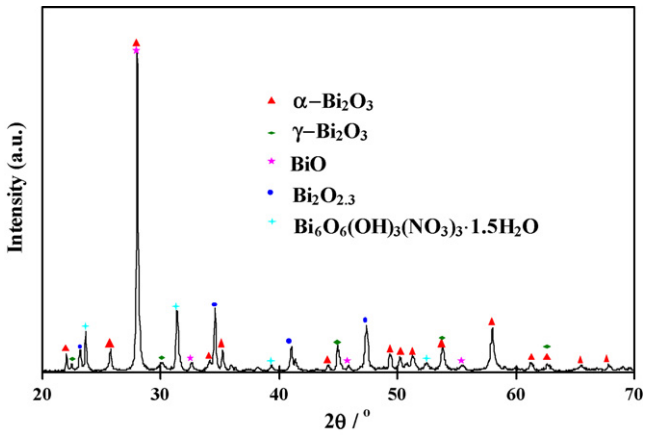

Fig. 1. X-ray diffraction pattern recorded from the as-synthesized bismuth oxide.

2.4. Preparation of enzyme electrodes

The BiO_x colloidal suspension (2 mg ml^{-1}) was prepared by dispersing BiO_x in deionized water with stirring overnight. PPO was also dissolved in deionized water with a concentration of 4 mg ml^{-1}. A defined amount of aqueous PPO/BiO_x mixtures (containing 40 μg PPO, 20 μg BiO_x) was spread on the surface of the glassy carbon electrode. The mixture was dried at room temperature, leading to a BiO_x film in which enzymes were entrapped. The resulting electrode was placed in saturated glutaraldehyde vapor at room temperature for 15 min in order to induce the chemical cross-linking of the entrapped enzyme molecules. Before use, the enzyme electrode was rinsed under stirring for 20 min with buffer solution to remove the enzyme not firmly immobilized.

3. Results and discussion

3.1. X-ray powder diffraction

The preparation method and conditions strongly influence the crystalline structure and phase composition of bismuth oxide films (Gotić et al., 2007), and thus we investigated the crystalline structure of the sample via XRD. Fig. 1 shows the typical XRD patterns of the as-synthesized bismuth oxide powder. XRD pattern of the sample was identified using data from JCPDS Powder Diffraction File (PDF cards). The XRD pattern shows formation of mixed phase of monoclinic α-Bi_2O_3 [PDF card No. 71-0465], body-centred cubic γ-Bi_2O_3 [PDF card No. 71-0467], BiO [PDF card No. 27-0054], nonstiochiometric $Bi_2O_{2.3}$ [PDF card No. 76-2477] along with the presence of bismuth oxide nitrate hydroxide hydrate [PDF Card No. 53-1038].

3.2. FTIR

The interaction between BiO_x and PPO molecules can be studied by comparing the IR spectra of the BiO_x, pure PPO, and PPO/BiO_x (Fig. 2). Fig. 2a shows the FTIR spectrum of the as-synthesized BiO_x. The vibration absorption bands due to NO_3^- (1373 cm^{-1}), Bi-O-Bi (810 cm^{-1}) and Bi-O (497 cm^{-1}) are observed (Irmawati et al., 2004). This suggests that as-synthesized BiO_x contains a large amount of NO_3^- groups, which are crucial for further surface functionalization and coating by any other functional groups (Yu et al., 2005). The IR spectrum of native PPO is illustrated in curve b of Fig. 2. The peak at 3288 cm^{-1} is assigned as N—H vibration of PPO. The peak at 2964 cm^{-1} is assigned as C—H vibration. Peaks from 1750 to 1600 cm^{-1}, from 1600 to 1500 cm^{-1} and from 1350 to 1200 cm^{-1} are assigned as amide I, amide II and amide III, respectively (Shi et al., 2003). When PPO was absorbed on BiO_x

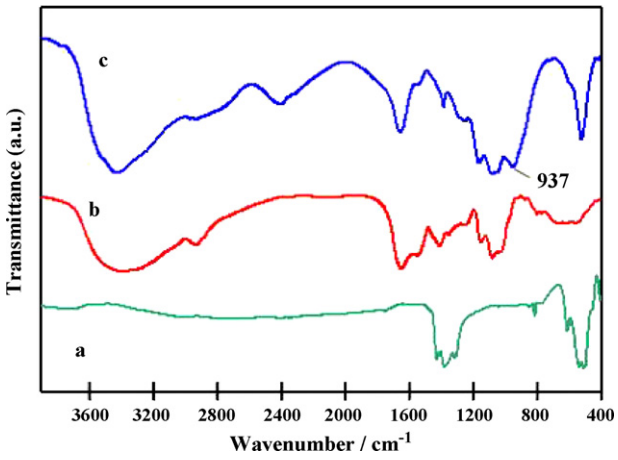

Fig. 2. FT-IR spectra of (a) BiO_x, (b) pure PPO, and (c) PPO-loaded BiO_x.

matrix, the relative intensity of the IR absorption between amide I and amide II bands of PPO is changed. The peak of amide II shifts slightly to the lower wavenumber (Fig. 2c). Moreover, a new absorption peak at 937 cm^{-1} is observed. These results indicate the binding of protein molecules to the mineral oxide surfaces.

3.3. Morphology of the as-synthesized BiO_x and PPO/BiO_x film

The surface morphologies of the membranes were examined by SEM imaging. The images (B and A) in Fig. 3 display the morphology of BiO_x films deposited with and without PPO molecules, respectively. The morphology of pure BiO_x film reveals a lamellar structure with thickness of 94.8–102 nm (Fig. 3A). BiO_x nanorods spread randomly can effectively increase the surface area, which is favorable for protein loading by physical adsorption. The inset of Fig. 3A displays the image of the initial droplet on pure BiO_x film. The contact angle of pure BiO_x was measured to be $48.2 \pm 0.5^\circ$, indicative for a hydrophilic surface. The hydrophilic BiO_x matrix is expected to provide a favorable microenvironment for the immobilized protein. In the case of PPO/BiO_x (w/w, 2), the BiO_x sheets are still observable with the increased thickness of 127–187 nm (Fig. 3B). The BiO_x sheets interconnect with each other and construct many cavities. Spongy-like materials can be found in the formed cavities. This porous structure would impart high diffusion rates of target analytes to a large number of accessible binding sites, which will be favorable for the design of the biosensor with high sensitivity (Walcarius, 2001).

3.4. Permeability of bismuth oxide modified films

The analytical performance for phenolic compounds developed by PPO/BiO_x electrode, such as response time and sensitivity, was expected to be strongly related to the permeation property of enzyme immobilization host matrix (Shan et al., 2003; Cosnier et al., 2006; Ionescu et al., 2004, 2005, 2006). Therefore, the mass-transfer process through PPO/BiO_x biomembrane to the surface of an electrode was investigated by rotating disk electrode voltammetry. Suppose that the charge density of BiOx is high, any charged molecule would affect the experimental results. Thus, the rotating disk voltammograms were obtained at PPO/BiO_x/GCE, BiO_x/GCE in an aqueous solution of a neutral molecule, hydroquinone (2 mM). The rotating disk voltammograms were also recorded from the bare glassy carbon electrode as a control electrode. The steady-state limiting current (i_{lim}) corresponding to the oxidation of hydroquinone was estimated to be 1.24, 1.17, 0.96 mA cm^{-2} for the bare GCE, PPO/BiO_x/GCE and BiO_x/GCE, respectively (Fig. 4). By comparing

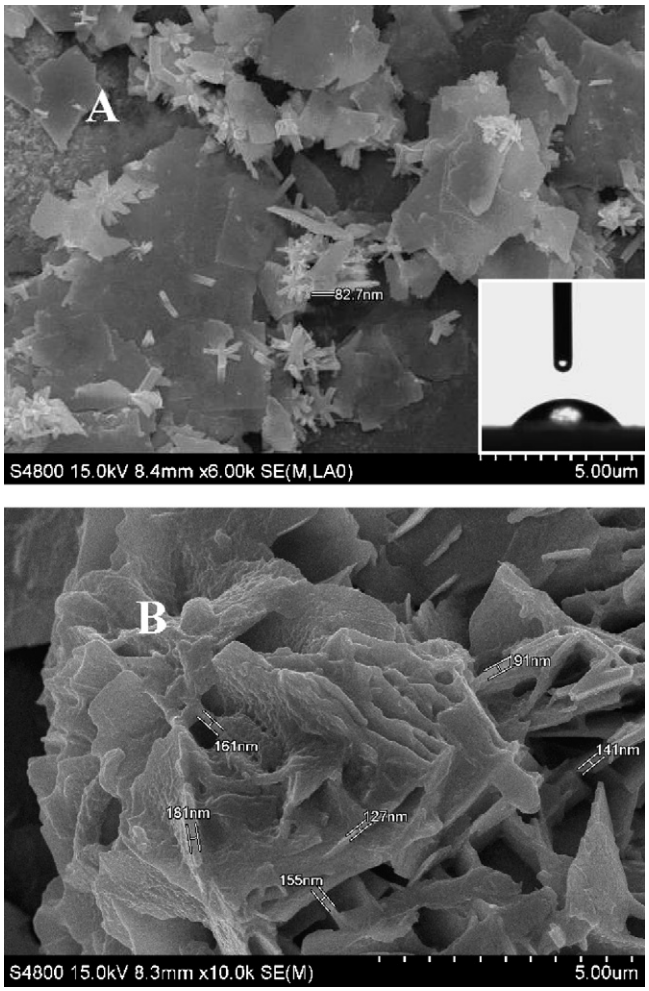

Fig. 3. SEM photographs of BiO_x (A) and PPO/BiO_x (w/w, 2) (B) films. Inset of (A) shows the image of the initial droplet on BiO_x film.

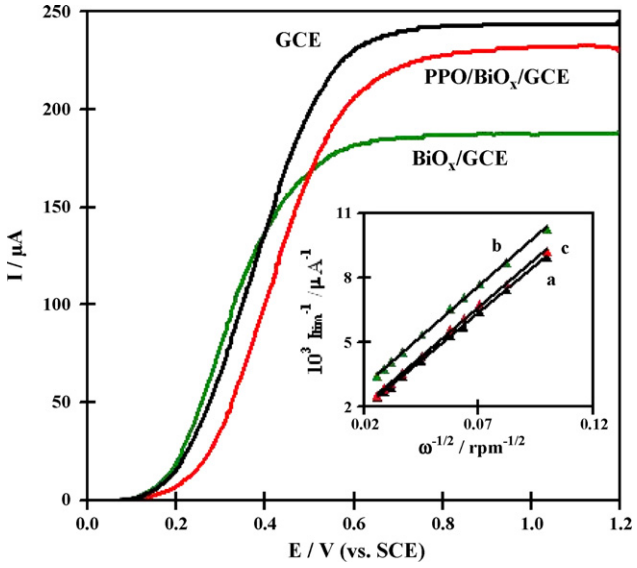

Fig. 4. Rotating-disk electrode voltammograms of GCE (5-mm, diameter), BiO_x/GCE and PPO/BiO_x/GCE in PBS (pH 6.0) containing 2 mM hydroquinone ($\upsilon = 10$ mV s^{-1}, $\omega = 500$ rpm). Inset: Koutecky–Levich plots for (a) GCE, (b) BiO_x/GCE, and (c) PPO/BiO_x/GCE.

the i_{lim} at the three different electrodes, BiO_x/GCE shows a higher diffusion resistance to the substrate than the PPO/BiO_x/GCE.

The permeability (P_m) of the PPO/BiO_x biofilm was determined from the typical equations introduced by Gough and Leypoldt (1979, 1980):

$$\frac{1}{i_{lim}} = \frac{1}{0.62\,nFAD_s^{2/3}C^0\nu^{-1/6}\omega^{1/2}} + \frac{1}{nFC^0AP_m}$$

where i_{lim} is the steady-state limiting current, A is the electrode area, D_s correspond to the diffusion coefficients of the substrate in the bulk solution, while C^0 the hydroquinone concentration, ν the kinetic viscosity of the solution, ω the rotation rate of the RDE.

To estimate the P_m value, Koutecky–Levich plots of $1/i_{lim}$ versus $1/\omega^{1/2}$ were made for the bare electrode and the electrode modified by PPO/BiO_x. The curve relative to the modified electrode presents a linear behaviour with the same slope to that obtained for a bare electrode with a positive intercept that depends on the permeability P_m of the biofilm (inset of Fig. 4). The estimated permeability of the PPO/BiO_x/GCE was calculated to be 8.26×10^{-2} cm s^{-1}, about 4.6 times greater than that of BiO_x/GCE (1.81×10^{-2} cm s^{-1}). Moreover, this permeability value obtained by PPO/BiO_x/GCE is much higher than those obtained by PPO/LDHs (2.5×10^{-2} cm s^{-1}) and PPO/laponite (6.6×10^{-3} cm s^{-1}) (Shan et al., 2003). This high permeability of PPO/BiO_x biomembrane may lead to the high and efficient mass transfer of the reactants and good accessibility of the immobilized enzymes, inducing the rapid and sensitive response to enzyme substrate (Wu and Choi, 2004).

3.5. Optimization of enzyme immobilization variables

The proportion between enzyme and BiO_x is the most significant process parameter for the performance of the biosensor. So the influence of the ratio (w/w) of PPO to BiO_x on the biosensor response was studied as the amount of enzyme being fixed at 40 μg. As expected, the biosensor response increases with the enzyme loading and then reaches a maximum for a PPO/BiO_x ratio of 2. For higher ratios, the amount of deposited PPO must exceed the retention properties of the BiO_x matrix, leading to an enzyme release.

The PPO/BiO_x ratio being fixed at 2, the effect of film thickness on the biosensor sensitivity was easily examined by varying the amount of PPO/BiO_x mixture deposited on the electrode surface. An initial increase in response was observed up to 40 μg PPO loading. Then, the biosensor response decreased with the increase in film thickness as previously observed for PPO-biosensors based on polymer films or inorganic coatings as the host matrix (Védrine et al., 2003; Shan et al., 2003; Han et al., 2007; Fan et al., 2007). This phenomenon was attributed to the fact that, for thicker films, most of the enzyme substrates (catechol and oxygen) were consumed at the matrix-solution interface. As a consequence, the majority of generated *o*-quinone was lost into the bulk solution instead of being reduced at the underlying glassy carbon electrode. Therefore, the configuration with a 40 μg PPO loading was chosen for the further experiments.

3.6. Optimization of detection test variables

The pH dependence of the PPO/BiO_x with the optimum configuration was investigated over the pH range 4–9 in 0.1 M PBS in the presence of 10 μM catechol. The optimum response current was found at pH 6, which is in good concordance with the optimum value found for PPO/laponite and PPO/layered double hydroxides (LDHs) coatings (Shan et al., 2003). This optimum value was situated in the pH range (5–8) reported for the free enzyme. This indicated that the immobilization procedure had not altered the optimum pH of PPO. Therefore, PBS at pH 6 was selected as the electrolyte in subsequent experiments.

The dependence of applied potential on the amperometric signal of the PPO/BiO_x sensor was also studied in this work. The current increased rapidly with the decreasing potential from 0.1 to −0.2 V and achieved maximum value at −0.2 V, while a small decrease in biosensor response was observed for more negative potentials. This may be attributed to an increase in the direct reduction of oxygen at the electrode surface, leading to the oxygen depletion within the biocoating and hence to a decrease in the enzymatic rate. Thus, −0.2 V was selected as the applied potential in subsequent experiments.

3.7. Enzyme electrode response characteristics

Under optimal conditions, the response time (defined as the time when 95% of the steady-state current is reached) was less than 8 s (see inset of Fig. 1S in the Supplementary data). Such a rapid response indicates a fast mass transfer of the substrate across the film and a fast electron exchange between PPO and its substrates, also indicating that the catalytic properties of the enzyme were not hindered by the BiO_x matrix. The proposed biosensor provides the linear range spans the concentration of catechol from 4 nM to 15 μM with a correlation coefficient of 0.999. Its sensitivity is 11.3 ± 0.2 A M^{-1} cm^{-2} (see Fig. 1S in the Supplementary data). This sensitivity for catechol is much higher than that of PPO immobilized in anionic clay layered double hydroxides (7.807 A M^{-1} cm^{-2}) (Shan et al., 2003), PPO entrapped in calcium carbonate nanoparticles (6.77 A M^{-1} cm^{-2}) (Shan et al., 2007), ZnO–sol–gel (2.4 A M^{-1} cm^{-2}) (Liu et al., 2005), and pyrrol–ammonium composite (1.5 A M^{-1} cm^{-2}) (Cosnier and Innocent, 1993). The excellent sensitivity of the PPO/BiO_x sensor may be ascribed to the merits of polycrystalline bismuth oxide film, such as high hydrophilic microenvironment, high permeability and excellent adsorption ability. In addition, the electrical resistivity measurements of bismuth oxide films exhibited a semiconducting behaviour (Gujar et al., 2006). Semiconductor BiO_x as enzyme immobilization matrix may lower the biomembrance resistance, which inducing the fast electron transfer.

Five phenolic compounds (catechol, *p*-cresol, phenol, *m*-cresol, *p*-chlorophenol), were monitored by the PPO/BiO_x electrode. Table 1 presents the response characteristics of the enzyme electrode including linear range, correlation coefficient, sensitivity, detection limit and the apparent Michaelis–Menten constant (K_M^{app}) for the different phenolic compounds. Response characteristics varied with the degree of substitution type and position of substitution. The sensitivity for the linear calibration regions follows this trend: *p*-cresol > catechol > *m*-cresol > *p*-chlorophenol > phenol.

This sequence is quite different from those reported for PPO based electrodes immobilized with anionic clay LDH (Shan et al., 2003), chitodan/laponite nanocomposite (Fan et al., 2007), $CaCO_3$ nanoparticles (Shan et al., 2007), and graphite–Teflon composite (Carralero et al., 2006). This seems to indicate a specific influence of the host matrix on the entrapped enzyme. Moreover, the K_M^{app} values obtained for *m*-cresol, *p*-cresol and catechol are 0.021, 0.036, 0.113 mM, respectively. These values are markedly lower than those reported for free enzyme (Barman, 1985). The lower K_M^{app} value may be ascribed to an efficient recycling substrate process, the electrochemical reduction of the enzymatically generated *o*-quinone, producing a hydroquinone derivative that is also PPO substrate (Shan et al., 2003). The phenolic compound enzyme recycling is dependent on the electrode matrix used (Serra et al., 2002). Thus, the immobilization of the PPO mentioned above appears to be beneficial to improve the biosensor's performance.

The reproducibility of the biosensor fabrication was evaluated via the comparison of the response current to 0.5 μM catechol of

Table 1
The response characteristics of the PPO/BiO_x bioelectrode to phenolic compound.

Phenol compound	Linear range (M)	R^2	Sensitivity ($A\,M^{-1}\,cm^{-2}$)	Detection limit (nM)	K_M^{app}(mM)
p-Cresol	1.3×10^{-9} to 4.0×10^{-6}	0.995	12.3	0.4	0.036
Catechol	4.0×10^{-9} to 1.5×10^{-5}	0.999	11.3	1.0	0.113
m-Cresol	1.0×10^{-9} to 4.0×10^{-6}	0.996	6.2	0.5	0.021
p-Chlorophenol	1.5×10^{-8} to 1.5×10^{-5}	0.996	3.9	5.0	0.435
Phenol	1.0×10^{-8} to 8.0×10^{-6}	0.998	3.2	5.0	0.319

different electrodes. Seven different enzyme electrodes were tested independently for the amperometric response to catechol, providing a RSD value of 5.6%. This indicates, in particular, an efficient and reproducible immobilization process of PPO in BiO_x matrix although the procedure used was a nonautomatic one.

The operational stability of the PPO/BiO_x electrode was also examined. A reproducible current response with a relative standard deviation (RSD) of 4.1% was observed in 40 successive assays of 0.5 μM catechol (see Fig. 2S in the Supplementary data). The stability of the PPO/BiO_x electrode stored at 4 °C was investigated by recording periodically its current response to 0.5 μM catechol. The response of the biosensor was unchanged during the initial three weeks. It still retained about 72% of its original response after 47 days of storage (see inset of Fig. 2S in the Supplementary data).

3.8. Interference studies

To evaluate the selectivity of the biosensor, the influence of some possible interfering substances were examined in PBS (pH 7.0) containing 0.75 μM catechol in the presence of different interferents, aniline, benzaldehyde, benzylalcohol, Mg^{2+}, Ca^{2+} and Cu^{2+}, each in concentration 100 times of that of catechol. The proposed sensor exhibited no significant interference in the presence of the aforementioned species, except in the case of benzaldehyde. Benzaldehyde, when present in a concentration of 1 mM, causes a slightly negative error, with average recoveries of 93.7%.

3.9. Analysis of real water samples

To study the real feasibility of the proposed biosensor, we checked the proposed biosensor in determination of catechol added to a matrix of natural river, using the standard addition method as reported previously (Kochana et al., 2008). The water samples were obtained from the local rivers (Slender Western Lake, Yangtze River and Jinghang Canal). No special sample pretreatment was performed-water samples were filtered and diluted threefold with buffer. The water samples were spiked with different amounts of catechol. The results of analysis obtained for different types of water are presented in Table 2. It is seen that, in general, the concentrations found were higher than those added. This indicates that the water matrix contained PPO substrates. For Slender Western Lake or Jinghang Canal, the excess of catechol found was lower than that for Yangtze River, indicating relatively better quality of water source. This is attributed to the effective environmental protection of Yangzhou city, which was awarded "Habitat Scroll of Honor" in 2006.

Table 2
Determination of spiked catechol in the matrix of natural waters.

Water sample	Catechol concentration		Recovery
	M (Added)	M (Found)	
Slender Western Lake	4.0×10^{-7}	4.2×10^{-7}	104.5%
	8.0×10^{-7}	8.2×10^{-7}	102.4%
	3.2×10^{-6}	3.4×10^{-6}	106.3%
	3.2×10^{-5}	3.4×10^{-5}	106.3%
	6.4×10^{-5}	7.0×10^{-5}	109.0%
Yangtze River	4.0×10^{-7}	4.6×10^{-7}	114.5%
	8.0×10^{-7}	1.0×10^{-6}	128.8%
	3.2×10^{-6}	3.8×10^{-6}	119.4%
	3.2×10^{-5}	3.6×10^{-5}	113.4%
	6.4×10^{-5}	7.8×10^{-5}	121.9%
Jinghang Canal	4.0×10^{-7}	4.2×10^{-7}	105.0%
	8.0×10^{-7}	8.2×10^{-7}	102.5%
	3.2×10^{-6}	3.4×10^{-6}	105.0%
	3.2×10^{-5}	3.2×10^{-5}	100.3%
	6.4×10^{-5}	6.8×10^{-5}	106.4%

4. Conclusion

In this study, a promising material, polycrystalline bismuth oxide, was firstly used as enzyme immobilization matrix for the biosensor construction. Due to the special properties of the bismuth oxide such as high surface activity, high dydrophilicity and biocompatibility, the entrapped PPO maintains its bioactivity. Thus, the proposed biosensor displays dramatically developed analytical performance over a wide linear range along with good stability and sensitivity. In addition, the porous structure of PPO/BiO_x film was expected to increase the accessibility to the substrate.

The structure and properties (electrical, optical, photoelectrical, etc.) of bismuth oxide depend on the synthetic approaches. Further work to study the different synthesis routes for different application of this material in direct electrochemistry, electrical and optical biosensing systems is currently on going and has achieved encouraging progress.

Acknowledgments

The authors are grateful to the financial supports of National Natural Science Foundation of China (Grant Nos. 20773108, 20505014 and 20810102052), Qing Lan Project of Jiangsu Province, China, the Institute of Ecology and Environment (Network Biosensors-Biofuel cells of the China-France program) from CNRS for partial financial support through the China-France program, and the project sponsored for D. Shan by the scientific research foundation for the returned overseas Chinese scholars, state education ministry. S.-N. Ding is grateful to the "Foundation Franco-Chinoise pour la Science et ses Applications" (FFCSA) for the postdoctoral fellowship and the Natural Science Foundation of Jiangsu (BK2007563) for financial support.

Appendix A. Supplementary data

Supplementary data associated with this article can be found, in the online version, at doi:10.1016/j.bios.2009.05.038.

References

Bagheri, H., Mohammadi, A., 2003. J. Chromatogr. A 1015, 23–30.
Bagheri, H., Mohammadi, A., Salemi, A., 2004. Anal. Chim. Acta 513, 445–449.
Barman, T.E. (Ed.), 1985. Enzyme Handbook, vol. 1. Springer-Verlag, New York, p. 226.
Carralero, V., Mena, M.L., Gonzalez-Cortés, A., Yánez-Sedeno, P., Pingarrón, J.M., 2006. Biosens. Bioelectron. 22, 730–736.
Cosnier, S., Innocent, C., 1993. Bioelectrochem. Bioenerg. 31, 147–160.

Cosnier, S., Mousty, C., Gondran, C., Lepellec, A., 2006. Mater. Sci. Eng. C 26, 442–447.
Fan, Q., Shan, D., Xue, H.G., He, Y.Y., Cosnier, S., 2007. Biosens. Bioelectron. 22, 816–821.
Faraji, H., 2005. J. Chromatogr. A 1087, 283–288.
Fu, J., 1997. J. Mater. Sci. Lett. 16, 1433–1436.
Gotić, M., Popović, S., Musić, S., 2007. Mater. Lett. 61, 709–714.
Gough, D.A., Leypoldt, J.K., 1979. Anal. Chem. 51, 439–443.
Gough, D.A., Leypoldt, J.K., 1980. Anal. Chem. 52, 1126–1130.
Gujar, T.P., Shinde, V.R., Lokhande, C.D., 2006. Mater. Res. Bull. 41, 1558–1564.
Han, E., Shan, D., Xue, H.G., Cosnier, S., 2007. Biomacromolecules 8, 971–975.
Ionescu, R.E., Gondran, C., Gheber, L.A., Cosnier, S., Marks, R.S., 2004. Anal. Chem. 76, 6808–6813.
Ionescu, R.E., Abu-Rabeah, K., Cosnier, S., Marks, R.S., 2005. Electrochem. Commun. 7, 1277–1282.
Ionescu, R.E., Herrmann, S., Cosnier, S., Marks, R.S., 2006. Electrochem. Commun. 8, 1741–1748.
Irmawati, R., Nasriah, M.N.N., Taufig-Yap, Y.H., Hamid, S.B.A., 2004. Catal. Today 93–95, 701–709.
Kochana, J., Gala, A., Parczewski, A., Adamski, J., 2008. Anal. Bioanal. Chem. 391, 1275–1281.
Li, W., 2006. Mater. Chem. Phys. 99, 174–180.
Liu, Z., Liu, B., Kong, J., Deng, J., 2000. Anal. Chem. 72, 4707–4712.
Liu, Z., Liu, Y., Yang, H., Yang, Y., Shen, G., Yu, R., 2005. Electroanalysis 17, 1065–1069.
Lupetti, K.O., Rocha, F.R.P., Fatibello-Filho, O., 2004. Talanta 62, 463–467.
Mailley, P., Cummings, E.A., Mailley, S.C., Eggins, B.R., McAdams, E., Cosnier, S., 2003. Anal. Chem. 75, 5422–5428.
Marlow, M., Hurtubise, R.J., 2004. Anal. Chim. Acta 526, 41–49.
Oliveira, H.M., Segundo, M.A., Reis, S., Lima, J.L.F.C., 2005. Microchim. Acta 150, 187–196.
PDF, cards No.: 71-0465; 71-0467; 27-0054; 76-2477; 53-1038, International Centre for Diffraction Data, Joint Committee on Powder Diffraction Standards, *Powder Diffraction File*, 1601 Park Lane, Swarthmore, PA 19081, USA.
Pocurull, E., Calull, M., Marce, R.M., Borrull, F., 1996. J. Chromatogr. A 719, 105–112.
Serra, B., Jiménez, S., Mena, M.L., Reviejo, A.J., Pingarrón, J.M., 2002. Biosens. Bioelectron. 17, 217–226.
Shan, D., Cosnier, S., Mousty, C., 2003. Anal. Chem. 75, 3872–3879.
Shan, D., Zhu, M.J., Han, E., Xue, H.G., Cosnier, S., 2007. Biosens. Bioelectron. 23, 648–654.
Shi, C., Liu, Q., Xie, Y., Xu, X., 2003. J. Mol. Struct. 644, 139–144.
Shuk, P., Wiemhöfer, H.D., Guth, V., Göpel, W., Greenblatt, M., 1996. Solid State Ionics 89, 179–196.
Switzer, J.A., Shumsky, M.G., Bohannan, E.W., 1999. Science 284, 293–296.
Védrine, C., Fabiano, S., Tran-Minh, C., 2003. Talanta 59, 535–544.
Wagner, L.K., 2007. J. Phys. Condens. Matter 19, 343201.
Wagner, L.K., Mitas, L., 2007. J. Chem. Phys. 126, 034105.
Walcarius, A., 2001. Electroanalysis 13, 701–718.
Wu, X.J., Choi, M.M.F., 2004. Anal. Chem. 76, 4279–4285.
Yu, M., Lin, J., Fang, J., 2005. Chem. Mater. 17, 1783–1791.